COMPDYN 2015
5th ECCOMAS Thematic Conference on
Computational Methods in Structural Dynamics and Earthquake Engineering
M. Papadrakakis, V. Papadopoulos, V. Plevris (eds.)
Crete Island, Greece, 25–27 May 2015

SHEAR HYSTERESIS MODEL FOR REINFORCED CONCRETE ELEMENTS INCLUDING THE POST-PEAK RANGE

Dimitrios K. Zimos[1], **Panagiotis E. Mergos**[1], **and Andreas J. Kappos**[1]

[1] Research Centre for Civil Engineering Structures, City University London
Northampton Square, London EC1V 0HB
e-mail: { Dimitrios.Zimos.1, Panagiotis.Mergos.1, Andreas.Kappos.1 }@city.ac.uk

Keywords: Earthquake Engineering, Non-ductile Reinforced Concrete Elements, Shear Hysteretic Behaviour, Post-Peak Response, Shear Failure, Loss of Axial Load Bearing Capacity.

Abstract. *Reinforced concrete (R/C) buildings designed according to older seismic codes represent a large part of the total building stock; hence, it is important to accurately and efficiently assess their response to actions induced by natural hazards, such as earthquake. Substandard R/C structural elements are prone to shear failure subsequent, or even prior, to yielding of their longitudinal reinforcement. This can potentially lead to loss of axial load bearing capacity of vertical elements and initiate progressive collapse of the building.*

So far, there have been efforts to model the full-range behaviour of such elements following a macro-modelling approach, usually based on quite a limited amount of experimental results, especially with respect to the post-peak part of their response, and adopting assumptions that are not entirely appropriate.

In the present study, an extensive database of shear and flexure-shear critical rectangular R/C columns has been compiled, to the purpose of investigating R/C member post-peak response and calibrating the models mentioned below. It includes both monotonic and cyclic tests, the latter constituting the majority, it spans a broad range of design, material and loading parameters and the majority of the specimens have been tested up to axial failure.

A shear macro-model is developed, which is able to capture the full hysteretic behaviour of R/C elements. In addition to the behaviour up to peak shear resistance, an effort is made to properly capture the post-peak response, calibrating an empirical model for the descending branch directly, instead of indirectly defining it through shear and axial failure that has traditionally been the case. The angle of the shear failure plane is an important parameter of this model, hence an empirical relationship has been developed for it, as well. The onset of axial failure constitutes a vital aspect of post-peak response, since it signals the initiation of a process of loss of an individual R/C element's axial load-bearing capacity simultaneously with the redistribution of vertical loads to neighbouring ones; thus, it was also closely examined and empirical models were derived.

1 INTRODUCTION

Reinforced concrete frame buildings designed according to older seismic codes (or even without adhering to any code) represent a large part of the total building stock. Transverse reinforcement in their structural elements is typically inadequate, widely spaced or poorly detailed, rendering them vulnerable to shear failure subsequent, or even prior, to yielding of their longitudinal reinforcement. This can eventually lead to loss of axial load capacity of vertical elements, through disintegration of the poorly confined concrete core and consequent axial load capacity decrease [1], and initiate vertical progressive collapse of a building. This collapse type has been shown through post-earthquake reconnaissance to be the most common reason of R/C frame building collapse, primarily due to failure of columns or beam-column joints [2]. Thus, it would be useful to be able to accurately and efficiently assess their response to earthquake-induced actions. Naturally, in such complex and computationally demanding analyses, especially when an attempt to model progressive collapse is made, the need for a macro-modelling approach of element behaviour arises.

2 CRITICAL REVIEW OF EXISTING MODELS

There have been several studies, especially in the recent years, attempting to model the full-range cyclic behaviour of shear-deficient elements. Some of the best-known models offer reasonable predictions of member response, but this is often not true in the post-peak range. In some cases, the post-peak descending branch is not explicitly considered, i.e. shear failure and axial failure models are calibrated and the descending branch is assumed to be the "connecting line" between these two, falling short of predicting the response measured experimentally (e.g. [3], [4]). Moreover, the shear strength is typically considered zero at the onset of axial failure - although this is not always the case, as will be shown later on, resulting in higher potential deviations. Another model [5] explicitly accounts for the post-peak descending branch, but is not calibrated against experimental results at all, thus being less accurate, as shown through the model verification against experimentally obtained results and noted by the authors; those that consider it directly and are indeed calibrated, are either associated with substantial scatter [6] or they neglect the effect of some critical parameters, such as transverse reinforcement [7]; furthermore, the datasets on which their empirical models were based are quite limited ([6], [7]), largely due to the scarcity of experimental tests of specimens up to the onset of axial failure until recently. Most of these constitutive models are based on inter-storey drift ratio (e.g. [3], [4], [7]), although it has been pointed out that a localised drift ratio (at the shear-damaged region) might be more appropriate, since deformations tend to concentrate at that region after shear failure [8]. Another shortcoming of some models is the consideration of a horizontal residual strength branch without solid experimental basis [6], [9], [10].

One of the most recent and comprehensive member-type models, which however does not cover the behaviour of R/C elements subsequent to the onset of shear failure, is the phenomenological, force-based, spread inelasticity model by Mergos & Kappos [11]–[13]. It is composed of 3 sub-elements, accounting for flexural, shear and anchorage-slip deformations (Figure 1). The shear sub-element primary V-γ curve includes the shear cracking point, the onset of yielding of the transverse reinforcement, where the maximum shear strength is attained, and a horizontal branch, where shear strains increase with constant force up to the onset of shear failure. The curve can be altered according to the flexural deformations in the plastic hinge zones, thus accounting for shear-flexure interaction.

The model was tested against different column specimens, which had failed in flexure, shear or flexure-shear, and adequate correlation was found. A specimen of interest for this

study in particular, i.e. a column specimen typical of buildings with inadequate transverse reinforcement [1], has been analysed using this model [14] and is presented herein. The analytical predictions are shown in Figure 2 along with the experimental results. The comparison with the experimentally observed behaviour up to the point of the onset of shear failure yields good accuracy.

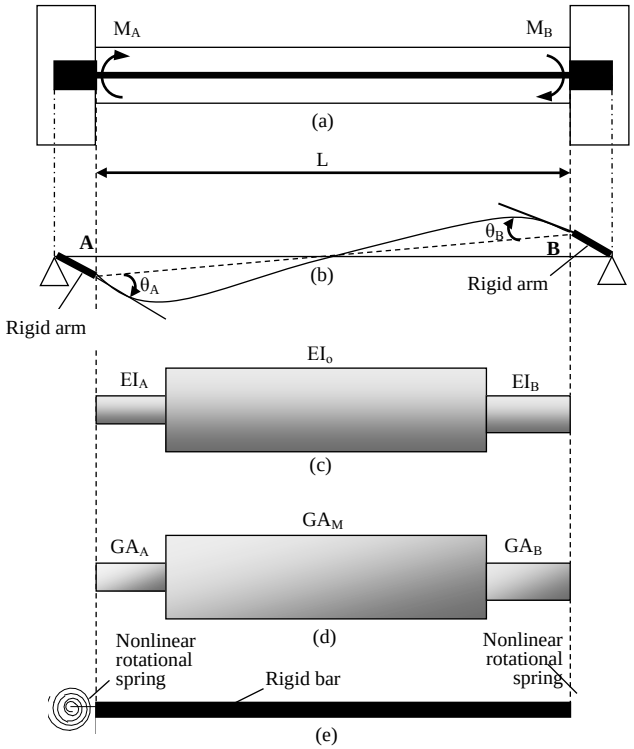

Figure 1: Finite element model: (a) geometry of R/C member; (b) beam–column finite element with rigid offsets; (c) flexural sub-element; (d) shear sub-element; (e) anchorage slip sub-element. [12]

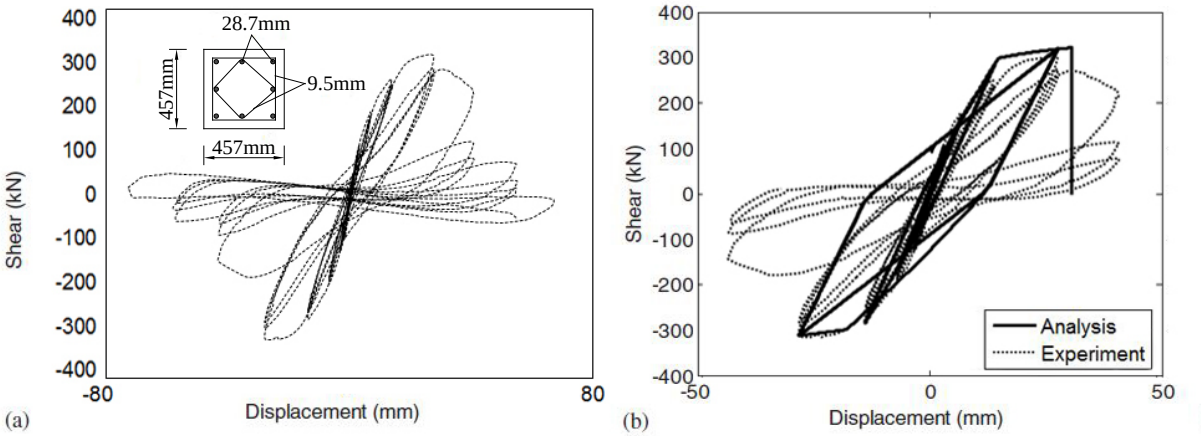

Figure 2: Sezen & Moehle [1] Specimen-1: (a) full lateral load vs total displacement hysteretic behaviour, as obtained from the experimental test; (b) lateral load vs total displacement hysteretic response resulting from analysis compared with the corresponding part of the experimental response [14].

Subsequent to the initiation of shear failure, the model is incapable of capturing the substantial strength degradation and follow the descending part of the response, which extends up to axial failure of the column. However, this part is critical in assessing the behaviour of an existing structure, even more so when it comes to predicting the initiation and cascade of pro-

gressive collapse in a building. Therefore, the primary aim of the present study is to incorporate post-peak shear strength degradation mechanisms to the existing member-type model, with a view to accurately capturing the response of shear-deficient elements up to the onset of axial failure.

3 POST-PEAK RESPONSE MODELLING

3.1 Database compiled

For the investigation of RC element post-peak response and the calibration of subsequent sub-models, a large database of shear and flexure-shear critical elements, which were cycled beyond the onset of shear failure, was compiled. It comprises 150 rectangular R/C columns, 67 of which have sustained flexure-shear failure and 83 failed in shear. Their main characteristics are summarised in Table 1.

	Min	Mean	Max
ρ_l (%)	0.16	2.25	4.76
ρ_w (%)	0.08	0.38	1.59
s/d	0.11	0.44	2.52
L_s/d	0.88	1.94	4.00
$\tau_{ave,max} / \sqrt{f_c}$	0.22	0.57	1.23
v	-0.26	0.26	0.80

Table 1: Main specimen characteristics of the database.

3.2 Modelling approach

The basic assumption adopted is that after the onset of shear or flexure-shear failure, the flexural and slip-induced deformations do not increase further than their values at failure, i.e. all post-peak deformations are localised in the shear sub-element. This assumption has been adopted in similar models (e.g. [4]) and is also experimentally validated through deformation decomposition (e.g. [15], [16]).

Furthermore, it has been observed that after the onset of shear failure, shear deformations tend to concentrate in a specific member region, the 'critical length' [8], [17]; this length is defined by the critical shear crack angle.

Based on the aforementioned assumptions, shear deformations are expressed as:

$$\gamma = \gamma_{sh,f} + \frac{\delta_{pp}}{L_{cr}} = \gamma_{sh,f} + \frac{\delta_{pp}}{h \cot \theta_{sh}} \quad (1)$$

where γ is the average shear strain in the critical zone, $\gamma_{sh,f}$ is the shear strain at the onset of shear failure, δ_{pp} is the post-peak total lateral displacement, L_{cr} is the critical length, h is the height of the section and θ_{sh} is the angle of the critical shear crack (with respect to the member axis).

The axial load capacity degrades with lateral displacement reversals, due to the disintegration of the confined concrete core [1]; the onset of axial failure is defined at the point where capacity and axial load demand become equal. It has long been claimed (e.g. [18]), based on limited amount of experimental data (e.g. [19], [20]), that axial failure occurs when shear

strength degrades to zero (or is at least negligible); many post-peak models have been based on this assumption (e.g. [3], [4]). Nonetheless, this can certainly not be assumed for all specimens. In fact, for some of them it's completely misleading and this can be readily shown in Figure 3, where the lateral strength at the onset of axial failure of the 88 specimens that have sustained axial failure in the database, is shown (normalised to the respective strength at shear failure, to get the residual lateral strength). Apparently, the shear strength of only a fraction of the specimens has degraded below 10% of the maximum strength.

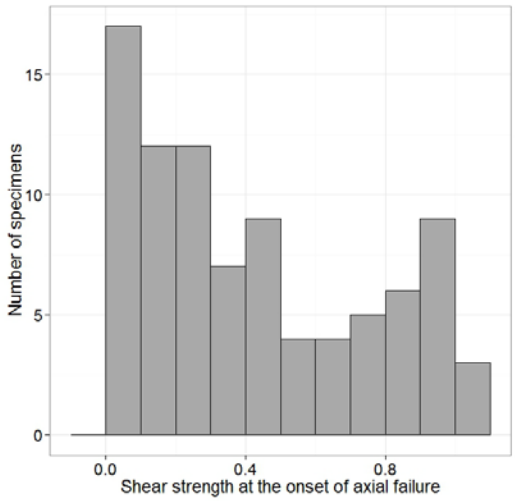

Figure 3: Distribution of the remaining shear strength (normalised by the maximum shear strength) at the onset of axial failure. The ostensibly extraordinary values near 1.00 are due to the inclusion of specimens having undergone simultaneous shear and axial failure.

Consequently, the assumption of zero strength at the onset of axial failure is not verified experimentally and will not be adopted in this model; instead, a displacement-based criterion will be sought. Simultaneously, of course, if the shear strength does indeed degrade to zero before this critical deformation is reached, that point will be considered the onset of axial failure, i.e. shear strength will not be allowed to assume negative values.

3.3 Critical crack angle

The critical shear crack angle has often been assumed independent of column properties (e.g. 45^o) in the process of developing a shear strength or an axial failure displacement model. As this angle affects (through L_{cr}) the modelling of the post-peak part of the shear force vs deformation curve, a realistic estimate of its value would be more appropriate; hence an appropriate model for this angle was sought.

It is first noted that this angle is not the angle of the first shear crack(s) that appear on a specimen along the principal compressive stress trajectories, when the tensile strength of concrete is reached. These can be readily calculated according to structural mechanics principles and result in steeper angles than the experimentally observed ones [8]. The critical shear crack angle corresponds to an idealised failure plane, which forms at or before shear failure and is different to the initial crack inclination.

Statistical analysis was performed on a subset of the database with either a given value of angle, or adequate photographic evidence to measure it directly; the crack angle was measured with respect to the longitudinal axis of the member. In the case of flexure-shear critical members with a fan-shaped crack pattern at the end-region, the steepest one was taken into account - being considered equivalent to the inclination of the crack that would form in the intermediate region without prior development of flexural hinges [21] -, disregarding potential

horizontal parts due to flexural cracking. Furthermore, cracks parallel to the longitudinal axis - usually caused by bond-split of the longitudinal reinforcement - were disregarded. Only double-curvature experiments were taken into account, since the few cantilever ones were observed to develop higher angle values which might not be representative of an actual building column. There were 51 shear critical (S) and 32 flexure-shear critical (FS) specimens satisfying the aforementioned criteria. Based on this dataset, the following patterns emerge (Figure 4):

- In line with structural mechanics principles, increasing axial load ratio (ν) tends to decrease the shear crack angle, since the trajectories of the principal compressive stresses - along which the first shear cracks will form – are oriented closer to the longitudinal axis of the member. The inclination of the shear failure plane, which is investigated herein, seems to have a similar correlation with the axial load ratio, being of course partly dependent on the initial shear cracks' inclination (it is emphasised again, though, that it forms generally at a different angle).
- Transverse reinforcement ratio (ρ_w) has a strong positive correlation with the angle. It is recalled that transverse reinforcement has hardly any influence on the principal stress trajectories prior to shear cracking, hence on the initial crack inclination. However, the angle of interest in the present model apparently includes the propagation of shear crack at varying angles, the angle change being significantly affected by the yielding transverse reinforcement.

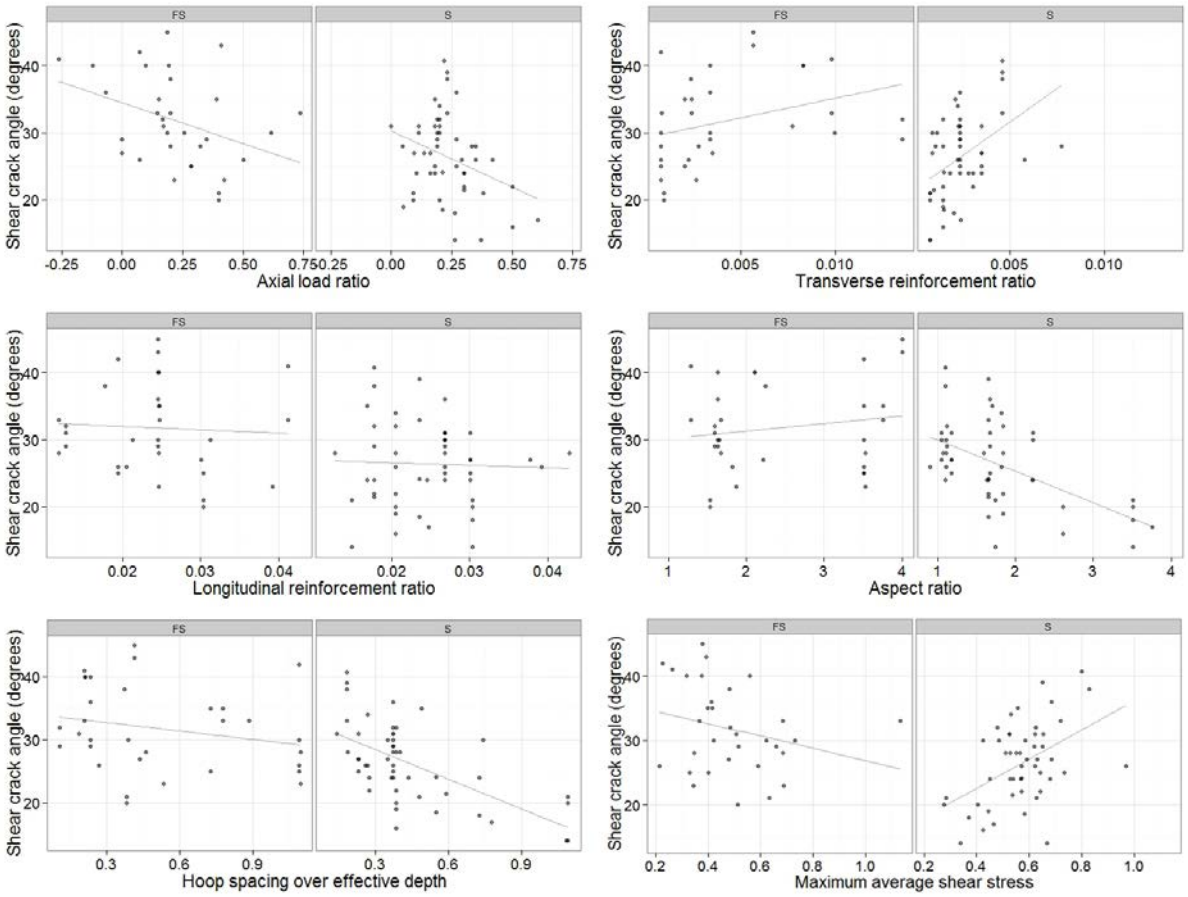

Figure 4: Correlation of the measured angle (in degrees) with axial load ratio (top left), transverse reinforcement ratio (top right), longitudinal reinforcement ratio (centre left), aspect ratio (centre right), hoop spacing over effective depth (bottom left) and maximum average shear stress (bottom right), divided into shear (S) and flexure-shear (FS) critical specimens.

- Longitudinal reinforcement ratio (ρ_l) seems to play no role whatsoever in either case (S or FS). This is consistent with the mechanics of shear cracking and contradicts previous studies (e.g. [21]) that have considered it as one of the main parameters.
- Aspect ratio (L_s/d) has a negative correlation in the case of shear critical elements, as expected, because of the influence on the trajectories of the principal compressive stresses. However, no definite trend was observed in flexure-shear critical elements, so no clear conclusions could be drawn.
- The normalised maximum average shear stress ($\tau_{ave,max} / \sqrt{f_c} = V_{max} / bd\sqrt{f_c}$) in S elements has the expected correlation according to the mechanics of cracking initiation, i.e. the higher the shear stress, the higher the angle. However, in FS specimens, the inverse seems to be the case.
- Hoop spacing over effective depth (s/d) has the inverse correlation of transverse reinforcement ratio, as expected, since the two parameters are highly correlated.
- In general, FS members seem to have higher shear crack angle values, the crack being confined in the end-region of the member that has yielded.
- Other important parameters that influence the shear crack angle, like cross-section shape and loading conditions, were beyond the scope of the current investigation, which was based on a database of only rectangular specimens - mainly square - and included only a double-curvature loading condition with forces acting at the ends of the members.

Existing shear crack angle models were tested against the experimentally measured values (Figure 5), to select an appropriate one to use in the context of the current model. Moharrami et al.'s model [22] is based on structural mechanics principles, hence the resulting angles are much steeper, in line with Elwood & Moehle's remarks [8]; this model was part of the development of a shear strength model, not a shear crack model per se. Chang's model [23] seems to heavily underestimate the angle, as well; probably because it's theoretically derived and not calibrated against experimental results, albeit not predicting the first shear cracks like the previous model. Ousalem et al.'s model [24] produces substantial scatter, largely attributed to the axial load ratio; both low and high values lead to great over- or underestimation, as it was developed based on specimens roughly in the range (0.05, 0.35). The only model which could decently represent the observed angles, is Kim & Mander's [21]. Still, it produces considerable scatter with a mean experimental-to-predicted value of 1.07 and a *CoV* of 23.9%, while it takes into account the longitudinal reinforcement ratio and disregards the effect of the axial load ratio.

Based on the aforementioned trends and significance tests of the predictor variables at a significance level of 5%, various empirical relationships were explored, since no existing model was deemed adequate. The best model developed is the following:

$$\theta_{\min} = \tan^{-1}\frac{h}{2L_s} < \theta_{sh} = \beta\frac{\rho_w^{0.14}}{\sqrt{\nu + 0.9}} < \theta_{\max} = 45^o \quad (2)$$

where β is a parameter that differentiates between shear and flexure-shear critical elements and is equal to 66 for S and 75 for FS elements and ρ_w is introduced with its actual value (not in %). The minimum value is a geometrical limitation of the shear crack applying to columns with a very low aspect ratio, as also explained by Elwood & Moehle [8]. Were this limit not imposed, the angle could be lower than the angle of the diagonal connecting the two ends of the column, essentially leading to an L_{cr} higher than the length of the column itself.

The model (Eq. 2) yields a mean experimental-to-predicted value of 1.00, a median of 0.97 and a Coefficient of Variation (*CoV*) of 19.6% (Figure 6). It applies to specimens in the fol-

lowing range of parameters: $-0.26 \leq v < 0.75$, $0.00 < \rho_w < 1.35$ (%), $1.18 \leq \rho_l \leq 4.28$ (%), $330 \leq f_{yl} \leq 700$ (MPa), $270 \leq f_{yw} \leq 587$ (MPa), $13.5 \leq f_c \leq 86$ (MPa), $0.9 \leq L_s/d \leq 4.0$.

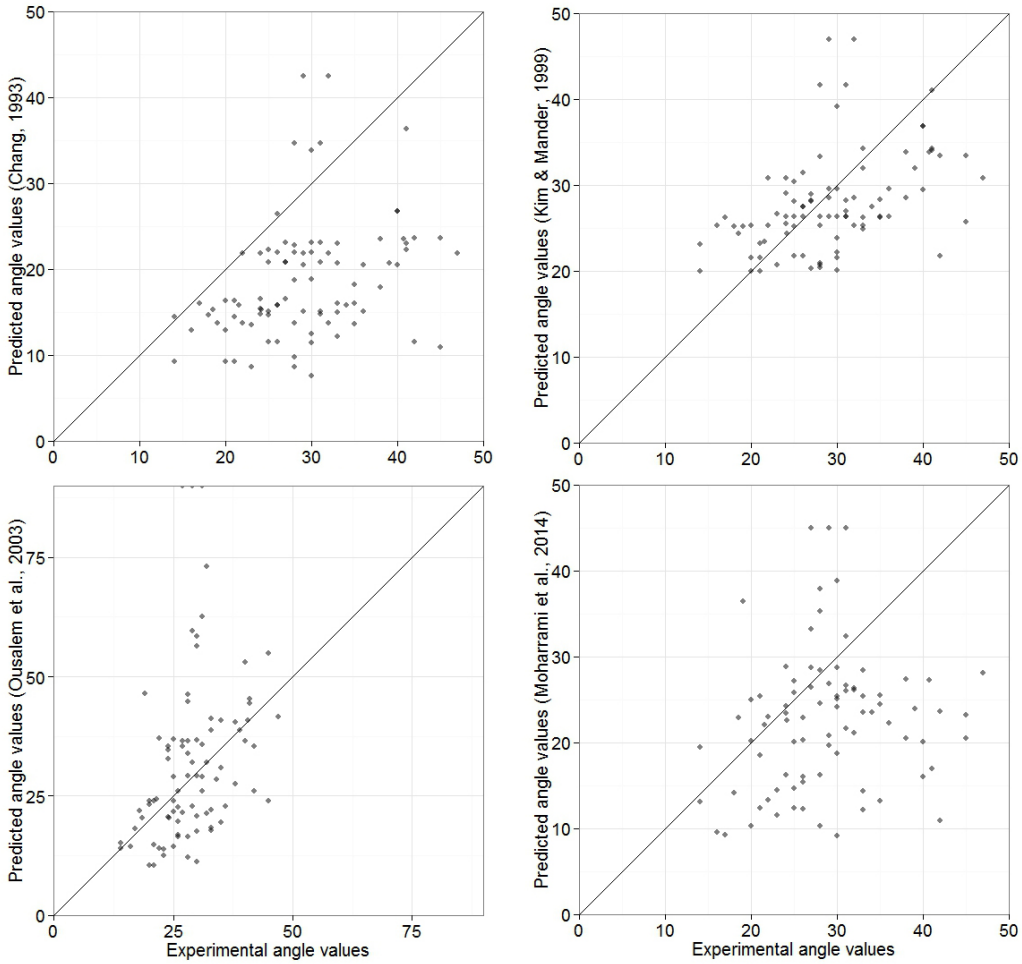

Figure 5: Shear crack angles (in degrees) measured experimentally against the ones calculated according to the predictive models of Chang [23] (top left), Kim & Mander [21] (top right), Ousalem et al. [24] (bottom left) and Moharrami et al. [22] (bottom right).

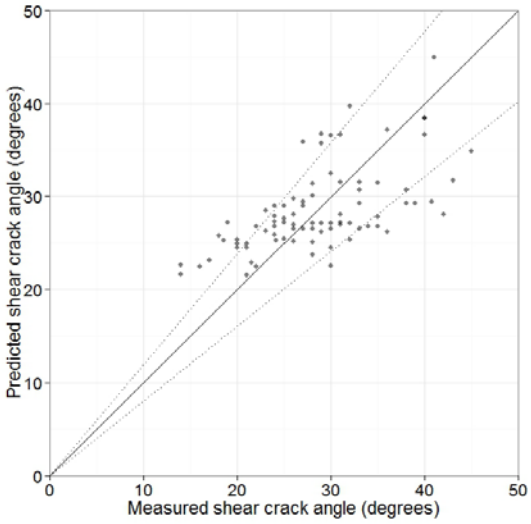

Figure 6: Shear crack angles (in degrees) measured experimentally against the ones calculated by the predictive model (Eq. 2).

3.4 Descending branch

With a view to developing a shear strength degradation model, the appropriate shape of the post-peak branch of the shear force vs deformation curve was investigated. From an observation-based classification, a bi-linear curve with a horizontal branch representing residual strength was a viable option for less than 10% of all specimens. This suggests either that practically no residual strength is developed in R/C members with the characteristics of this database, or that axial failure occurs in most specimens before they reach their residual capacity. Another option could be a non-linear branch, which would have to encompass both concave and convex degradation curves. However, a linear post-peak branch model was pursued, taking into account its simplicity, its compatibility with existing shear behaviour macro-models and its match with the experimental results, with the Coefficient of Determination (R^2) of fitting a linear least-squares line to the experimental post-peak response of each individual specimen of the database having an average value of 0.95 and a Coefficient of Variation (*CoV*) of 7.43%. Thus, the proposed strength degradation model is the following:

$$\frac{V}{V_{\max}} = 1 - S_{pp}(\gamma - \gamma_{sh,f}) \tag{3}$$

where V_{max} is the maximum shear strength that occurs at the onset of shear failure, $\gamma_{sh,f}$ the corresponding shear strain, $\gamma \geq \gamma_{sh,f}$ and $V \leq V_{max}$ the shear strain and strength at any loading level after shear failure and S_{pp} the slope of the post-peak curve, i.e. the rate of shear strength degradation (see Figure 7).

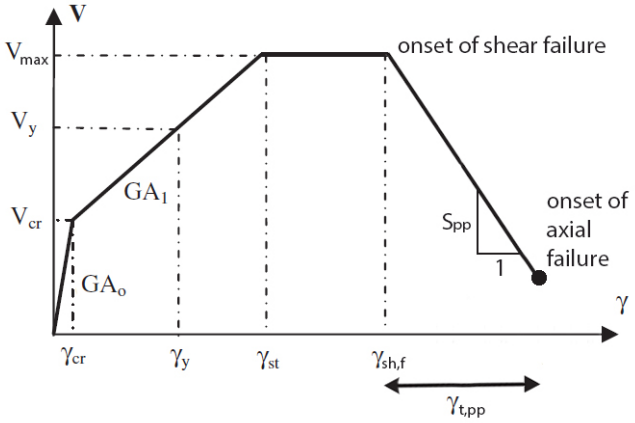

Figure 7: V-γ primary curve including the post-peak range (without shear-flexure interaction).

The post-peak behaviour of specimens with a degradation of at least 30% of V_{max} was considered, in order to obtain a genuine descending branch in the response. Thus, experiments that were conducted up to 85% or 80% of V_{max}, which constituted the overwhelming majority until recently, were excluded. The critical crack angle - for the calculation of the critical length and the normalisation of the lateral displacements - was calculated according to the aforementioned predictive model (Eq. 2). The principal direction, i.e. the direction of shear failure occurrence, was considered only, since the other one is influenced by the preceding shear failure, so it is not necessarily identical to the principal one.

Considering the slope of monotonic and cyclic specimens with various lateral displacement protocols (47 flexure-shear and 71 shear critical specimens) led to excessive scatter; for example, the best models would hardly amount to an R^2 of 0.45 and a *CoV* less than 60%. Furthermore, lumping them all together would lead to confusion between the capacity boundary of monotonic specimens as well as those with large displacement reversals and the cyclic en-

velopes of cyclic specimens with smaller reversals, hence confounding in-cycle with cyclic degradation. It has been pointed out theoretically that these degradation types should be separated (e.g. in FEMA P440A [25]); it was also proven experimentally, for example by observing the apparent difference in the descending branch slope of the identical specimens D13 and D14, which were cycled following different loading protocols [26]. Therefore, it was decided to treat them separately. A fraction of the specimens was selected, which were either monotonic or cyclic with very large lateral displacement reversals (exhibiting apparent in-cycle degradation). These amounted to a total of 28, 18 of which were shear critical and 10 flexure-shear.

Examining the correlation of the descending branch slope (in a curve depicting V/V_{max} vs γ) with design and loading parameters (Figure 8), the following are observed:

- Higher axial load ratio increases the post-peak slope, as has been often noted in similar studies (e.g. [7]). Naturally, it leads to higher stresses along the inclined crack interface, causing faster deterioration of shear resisting mechanisms, albeit increasing shear friction at the same time.
- Higher longitudinal reinforcement is beneficial, decreasing the degradation rate, mainly through the dowel action of the longitudinal bars as well as carrying a - potentially significant - part of the vertical load, hence reducing the damage inflicted on the crack interface during each reversal. Interestingly, the longitudinal reinforcement area normalised by the confined section area gives a better prediction than when normalised by the entire section area, the latter being the usual variable of preference in pre-peak models. This is possibly due to the fact that after the critical shear crack has formed at the onset of shear degradation, the effective area is the confined one, as the unconfined cover concrete either has already failed due to spalling of the section at the member critical length or it does not actively contribute as resistance mechanism, due to substantial reduction in its strength.
- Higher transverse reinforcement is beneficial, as expected, as the transverse steel bars crossing the critical crack are one of the main resistance mechanisms.
- The average diameter of longitudinal bars (normalised by the effective depth, to avoid scaling issues), $\Phi_{l,ave}/d$, seems to play an important role, too. The same longitudinal reinforcement ratio realised through less bars of larger diameter will increase the shear resisted by dowel action.
- Aspect ratio is an important parameter of a member's shear behaviour, but was found not to hold high predictive strength herein. This is due to the fact that shear strains concentrated in the critical length were considered, therefore eliminating the effect of aspect ratio, which is pronounced when taking into account the inter-storey drift ratio (e.g. in [7]).

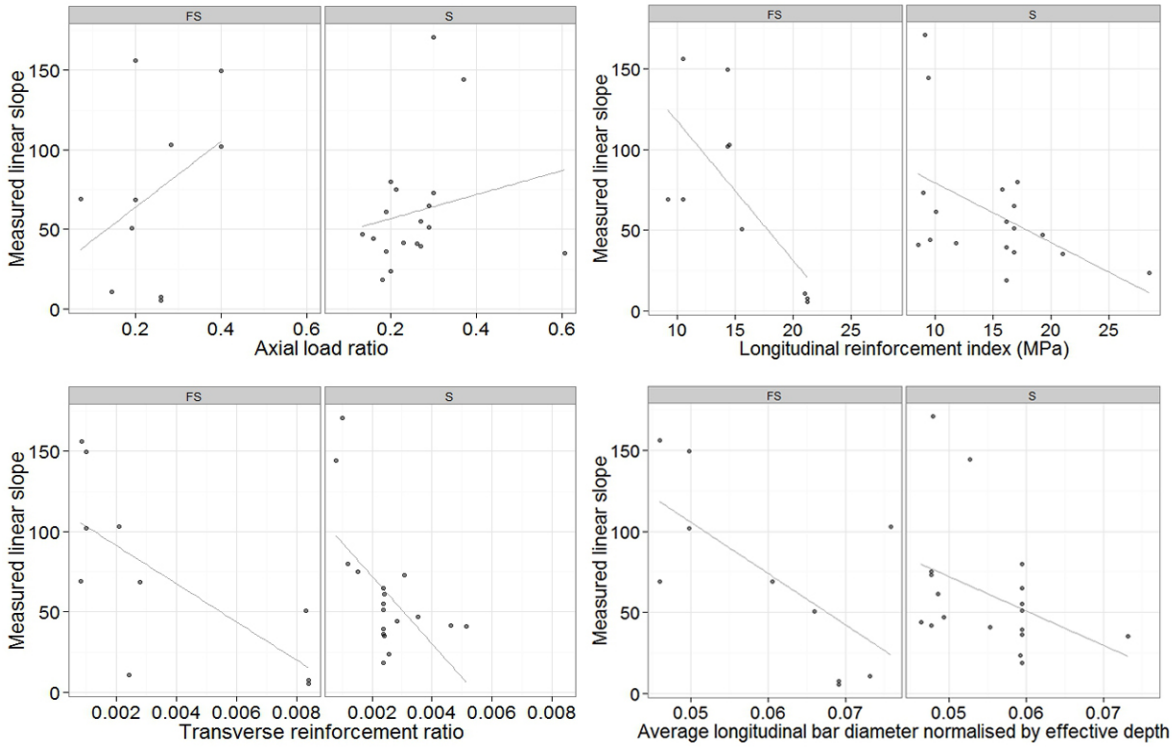

Figure 8: Correlation of the measured slope of the linear post-peak branch with axial load ratio (top left), longitudinal reinforcement index (top right), transverse reinforcement ratio (bottom left), average longitudinal bar diameter normalised to the effective depth (bottom right), for shear (S) and flexure-shear (FS) critical specimens.

Based on these trends and significance tests of the predictor variables at a significance level of 5%, various empirical models were explored. The best predictive model was the following:

$$S_{pp} = 7.36 + \frac{0.28\sqrt{\nu + 0.02}}{\left(\rho_w + 0.0011\right)\left[\frac{\rho_l f_{yl}}{A_{conf,\%}}\left(\frac{\Phi_{l,ave}}{d}\right) + 0.06\right]} \quad (4)$$

where ρ_w and ρ_l are introduced with their actual value (not in %) and f_{yl} in MPa. This model yields an R^2 of 0.82, which is considered quite high, taking into account the high uncertainty inherent in post-peak phenomena (for instance, the effect of experimental set-up and the randomness of the succession of degrading phenomena taking place at a lower level) as well as comparing it with existing models (e.g. R^2 of 0.6 in [6]). The mean experimental-to-predicted value is 1.00 and the median 0.87 (Figure 9). It can be applied to specimens in the ranges: $0.05 \leq \nu \leq 0.60$, $0.00 < \rho_w < 0.85$ (%), $0.045 \leq \Phi_{l,ave}/d \leq 0.075$, $1.50 \leq \rho_l/A_{conf,\%} \leq 4.30$ (%), $330 \leq f_{yl} \leq 700$ (MPa), $270 \leq f_{yw} \leq 587$ (MPa), $13.5 \leq f_c \leq 86$ (MPa), $1.1 \leq L_s/d \leq 3.8$.

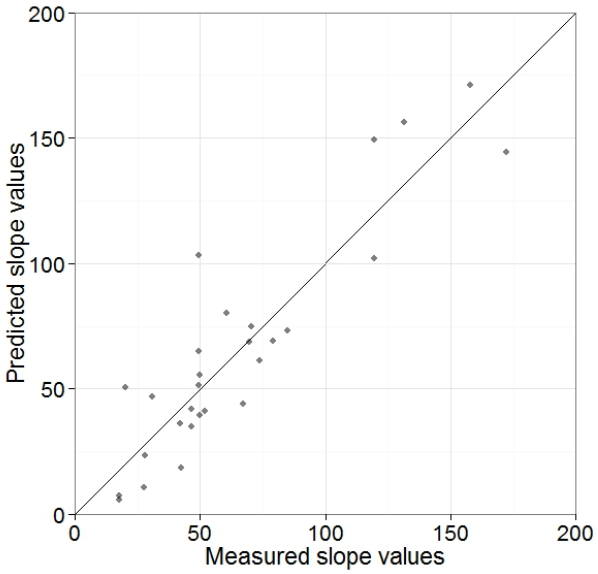

Figure 9: Values of the post-peak descending branch slope (dimensionless) measured experimentally against the ones calculated using the predictive model (Eq. 4).

3.5 Axial failure

Existing models predicting the lateral displacement at the onset of axial failure were applied in this extensive dataset of 88 specimens having sustained axial failure, to find the most accurate one to employ. Nonetheless, their predictive ability was not adequate (Figure 10). Ousalem et al. and Yoshimura models [26], [27] seem to systematically overestimate the lateral displacement. Matamoros & Von Ramin model [28], on the other hand, seems to systematically underestimate it. Elwood & Moehle, Zhu et al., and Wibowo et al. models [7], [8], [29] seem to capture the displacements on average, albeit exhibiting very high scatter. Most of these models ([8], [26], [28], [29]) apply only to flexure-shear critical specimens. Furthermore, all of them but one [7] are based on a rather limited dataset.

Consequently, it was decided to develop a new empirical model that would accurately capture the trends observed in this dataset and would fit with the shear model of this study.The variable chosen to fit the shear model - and because it correlates better with predictive variables - was the following:

$$\gamma_{t,pp} = \frac{\delta_{ax,f} - \delta_{sh,f}}{L_{cr}} \tag{5}$$

where $\gamma_{t,pp}$ is the total post-peak shear strain (see Figure 6), $\delta_{ax,f}$ is the lateral displacement at the onset of axial failure, $\delta_{sh,f}$ is the lateral displacement at the onset of shear failure and L_{cr} is the already mentioned critical length, where shear strains concentrate after the onset of shear failure.

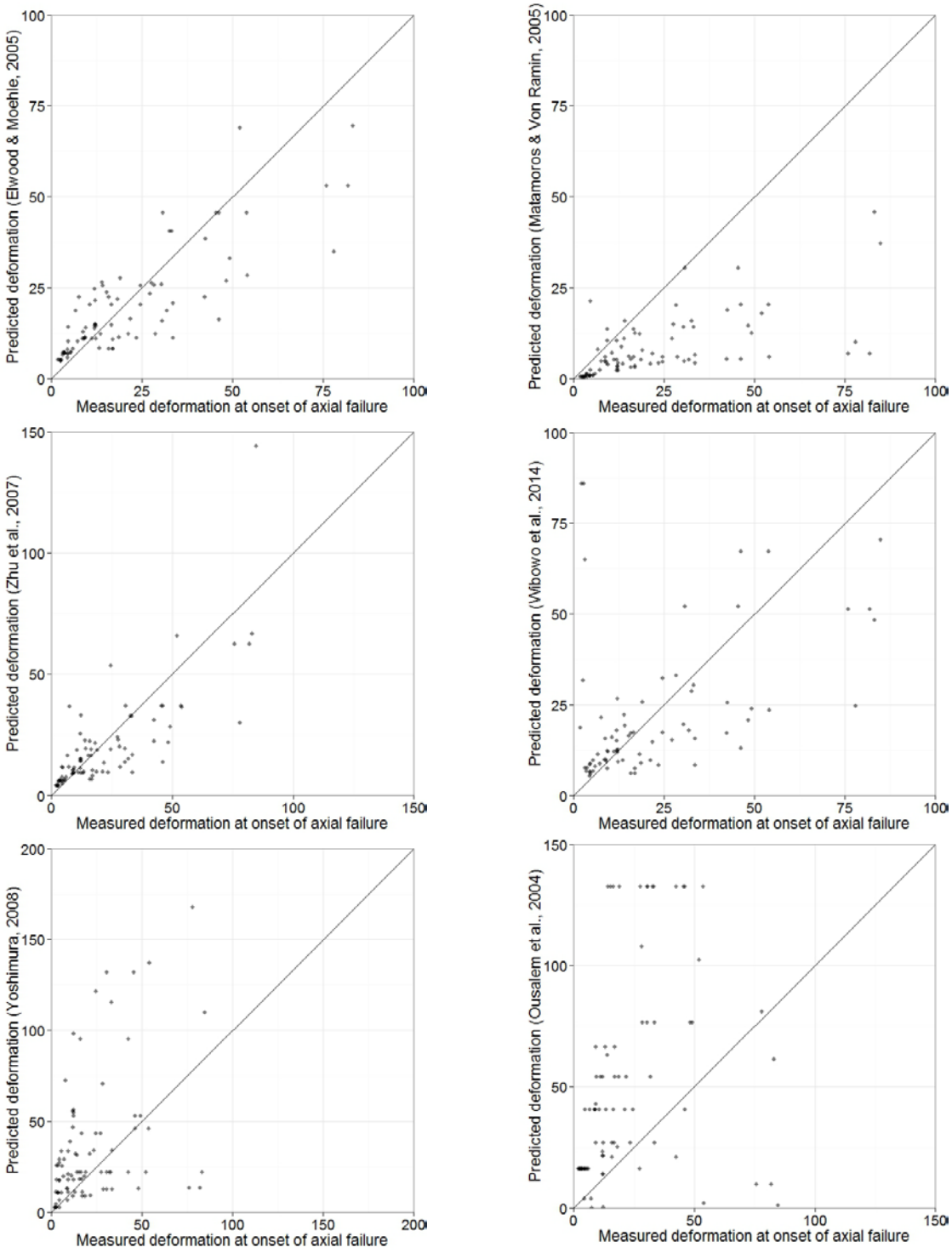

Figure 10: Existing models of lateral displacement at the onset of axial failure applied in the specific database. The measured displacements lie on the horizontal axis, while the predicted ones on the vertical. The plotted line is the "identity" line, i.e. where these two would be exactly equal. The models depicted are: Elwood & Moehle [8] (top left), Matamoros & Von Ramin [28] (top right), Zhu et al. [29] (centre left), Wibowo et al. [7] (centre right), Yoshimura [27] (bottom left) and Ousalem et al. [26] (bottom right).

Examining the correlation of the total post-peak shear strain with design and loading parameters (Figure 11), the following are observed:

- Axial load ratio is a pivotal parameter, decreasing the member's deformability, as has been noted time and time again in similar studies (e.g. [1], [7], [8], [30]). Interestingly enough, the axial load ratio was found much less significant than the longitudinal reinforcement axial load ratio ($\nu_l = P / (A_{sl} f_{yl})$), which was proposed as a predictor in a previous study [19], so the latter was used in model development herein.

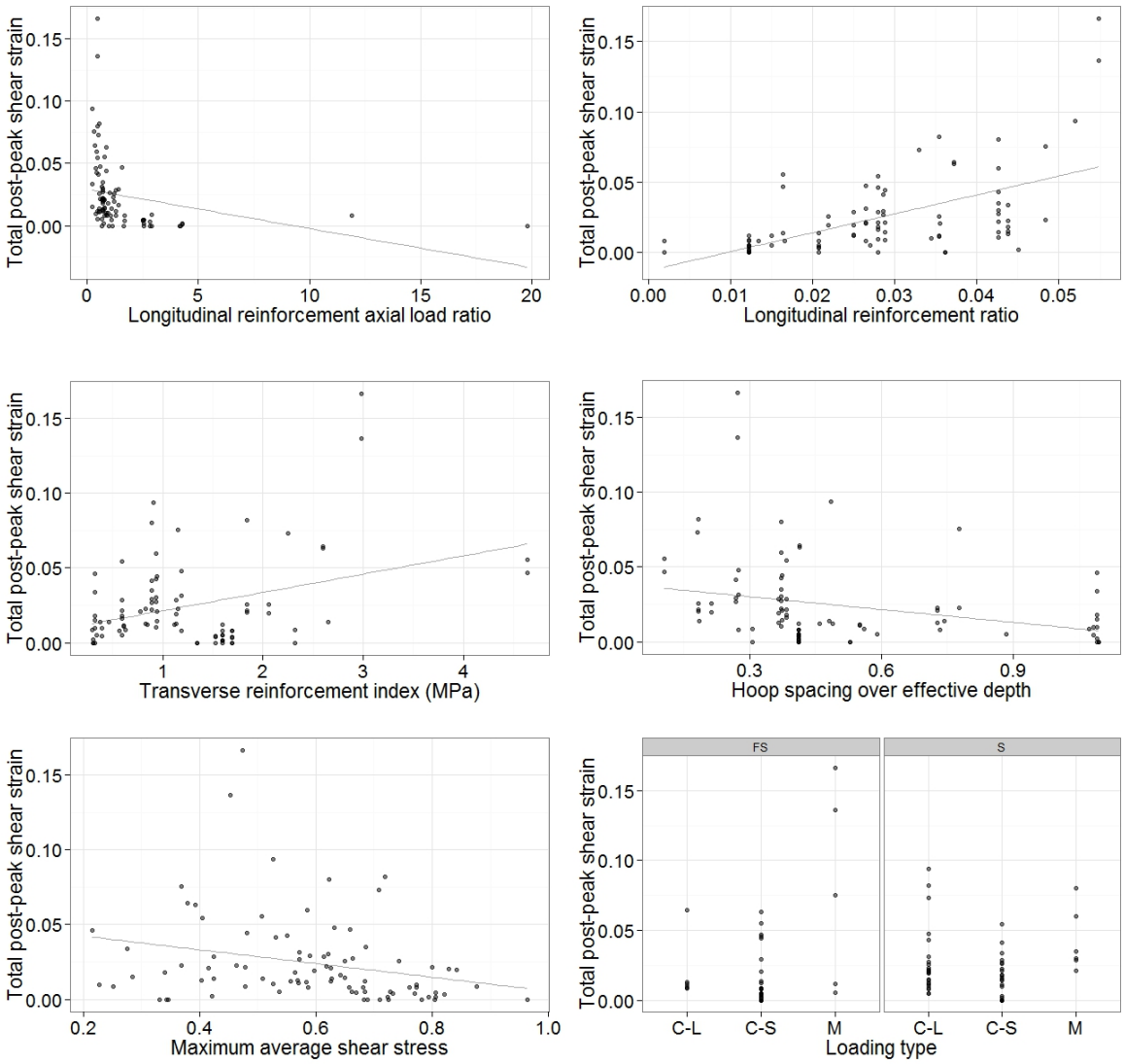

Figure 11: Correlation of the total post-peak shear strain at the onset of axial failure (derived from the experimentally measured values and based on the abovementioned angle model, Eq. 2) with axial load ratio based on the capacity of the longitudinal reinforcement (top left), longitudinal reinforcement ratio divided by the percentage of confined area (top right), transverse reinforcement ratio multiplied by its yield strength (centre left), hoop spacing over effective depth (centre right), maximum average shear stress (bottom left) and the loading type, divided into shear (S) and flexure-shear (FS) critical specimens (bottom right).

- According to these data, it seems that simultaneous shear and axial failure does not necessarily occur when the aforementioned ratio is higher than unity, some of these specimens reaching a total post-peak shear strain of 0.047; however, in specimens with a ratio higher than two, it was in every case less than 0.01 and mostly zero, indicating that this could be an appropriate threshold for certain simultaneous shear and axial failure. However, this should not be the only criterion, since there are even specimens with a ratio

lower than unity, which have experienced such failure. Each of these specimens, though, had a ratio higher than 0.65, in line with observations of a previous study [31].

- Higher longitudinal reinforcement is beneficial, increasing the post-peak deformability, as observed in previous studies [19], [31]. Longitudinal bars take up part of the axial load, partially relieving the confined concrete core from damage inflicted by the displacement reversals. Also, it allows for redistribution of a higher percentage of the axial load from the concrete in later stages.
- Naturally, transverse reinforcement is beneficial, as underlined repeatedly in the past (e.g. [8], [17], [27], [30]). It confines the concrete core, allowing for higher load capacity and takes up a significant part of the shear demand, decreasing the shear strength degradation of the member and the damage inflicted to the core along the shear failure plane.
- Lower hoop spacing decreases the buckling potential of longitudinal bars and increases the confinement of the core, even with constant transverse reinforcement ratio, hence increasing deformability. This has led to appreciating that larger ties at larger spacing lead to lower deformability (e.g. [17]).
- The higher the average shear stress at the point of maximum lateral loading - causing more damage, hence higher degradation -, the lower the achieved deformation at the onset of axial failure, as expected.
- It has been noted several times that monotonic response (M) leads to higher deformability than the cyclic one (e.g. [1], [19]). From the correlations, it seems that also the cyclic specimens with large displacement reversals (C-L), so large that in-cycle degradation is obvious, have also higher deformation capacity, as compared with the ones with small reversals and no in-cycle degradation (C-S). A simplified parameter is introduced herein to account for this effect, in lack of series of experimental tests with various displacement protocols, so as to investigate this issue in depth.
- Flexure-shear critical specimens (FS) seem to exhibit higher deformability on average, when contrasted to shear-critical ones (S).

Based on these trends and significance tests of the predictor variables at a significance level of 5%, various empirical relationships were explored. The best models developed are the following two:

$$\gamma_{t,pp} = 2.2 F_t L_t \frac{\rho_l}{\sqrt{\nu_l A_{conf,\%}}} \sqrt[3]{\frac{\rho_w f_{yw}}{s/d \; f_c}} - 0.005 \geq 0 \tag{6}$$

$$\gamma_{t,pp} = 0.65 \left(\frac{\rho_l}{A_{conf,\%}} \right)^{1.2} \sqrt{\frac{\rho_w f_{yw}}{\nu_l \, s/d \; \tau_{ave,max} / \sqrt{f_c}}} \geq 0 \tag{7}$$

where F_t is a parameter that differentiates between shear and flexure-shear critical elements and is equal to 1 for S and 1.07 for FS elements, L_t is equal to 1 for cyclic displacement protocols and 1.35 for monotonic response and ρ_l, ρ_w are introduced with their actual value (not in %). The first model (Eq. 6) yields a mean experimental-to-predicted value of 1.04, a median of 0.94 and an R^2 of 0.84, while the second one (Eq. 7) 1.02, 1.02 and 0.83 (Figure 12).Both models apply to specimens in the following range of parameters: $0.07 < \nu < 0.66$, $0.00 < \rho_w \leq 1.35$ (%), $0.15 < \rho_l \leq 3.8$ (%), $331 \leq f_{yl} \leq 700$ (MPa), $303 \leq f_{yw} \leq 587$ (MPa), $13.5 \leq f_c \leq 33.6$ (MPa), $1 < L_s/d \leq 4.25$.

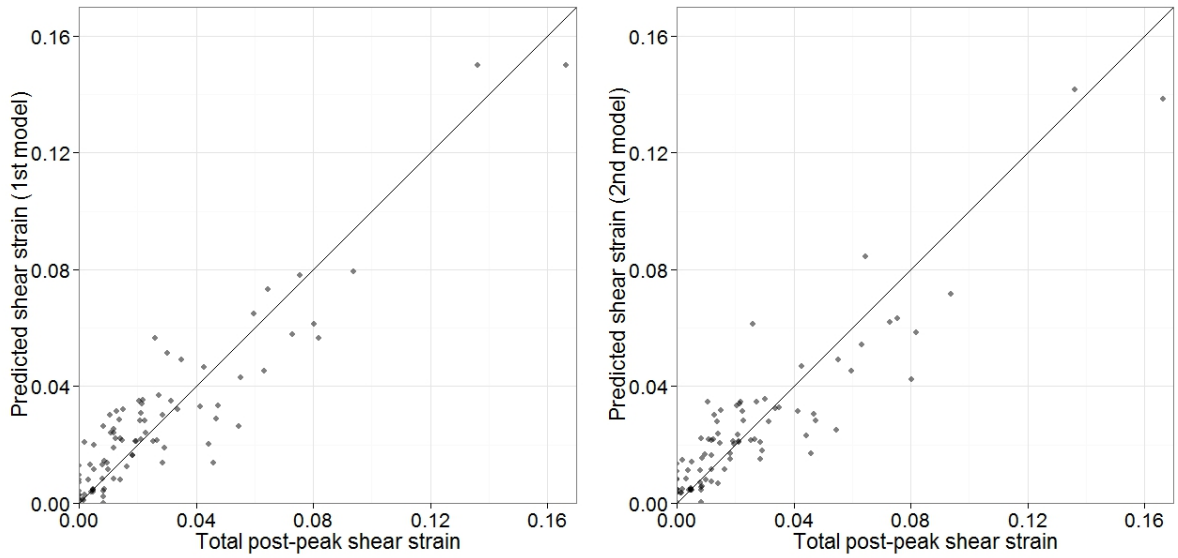

Figure 12: Values of the total post-peak shear strain at the onset of axial failure (derived from the experimentally measured values and based on the abovementioned angle model, Eq. 2) against the ones calculated using the 1st predictive model (Eq. 6) (left) and the 2nd one (Eq. 7) (right).

4 CONCLUSIONS

The post-peak response of shear-deficient members was the focus of this study. This is the core of the effort to extend the capabilities of an existing efficient member-type model [12], with a view to reliably capturing the full-range response of such members. From a rather large database of rectangular shear and flexure-shear critical specimens that was compiled, it was found that the best modelling approach for the post-peak descending branch of the shear force vs deformation curve is a straight line, due to its simplicity, compatibility with other existing models and matching the experimentally determined response.

A predictive model for the critical shear crack angle of an R/C member, which differentiates between shear and flexure-shear critical elements, is put forward. It was found to yield rather accurate predictions and it was used for the development of the subsequent models. Decreasing axial load ratio, as well as increasing transverse reinforcement ratio, lead to an increase in the critical angle, influencing the initiation and propagation of shear cracks, respectively. The longitudinal reinforcement ratio was found to have no effect, despite having been considered influential in previous studies. The change in shear crack propagation as the failure type changes from shear to flexure-shear leads to larger angles in the latter case, as well as inverse correlation of the angle with the aspect ratio and the maximum average shear stress.

A model for the linear degradation rate of shear strength as deformation increases was also developed. It was found to be very accurate, considering monotonic and cyclic specimens with large displacement reversals. Higher transverse and longitudinal reinforcement ratios, longitudinal reinforcement yield strength, and average diameter of longitudinal bars have a beneficial effect, reducing the shear strength degradation rate. On the other hand, increasing axial load ratio leads to more pronounced strength degradation. The aspect ratio does not have a significant effect in this model, largely due to the assumption that post-peak shear strains are concentrated within a critical length, rather than being evenly distributed along the R/C member.

Shear strength has been typically considered zero at the onset of axial failure, due to extensive degradation, based on a limited pool of experimental results. It was demonstrated herein

that this is usually not the case, thus it cannot always be considered a valid assumption. This, of course, does not imply a residual lateral strength during (or after) axial failure; that is a separate matter to be further investigated.

Two alternative predictive models are put forward among those developed for the total post-peak shear strain of an R/C member. They are considered accurate in the context of the phenomenon under study, the latter model being more parsimonious. This strain is found to positively correlate with transverse and longitudinal reinforcement, smaller hoops spaced more closely and lower axial and shear loads. Moreover, members that fail in shear after prior yielding of longitudinal reinforcement, as well as members loaded monotonically or undergoing larger - and fewer - displacement cycles seem to reach higher deformation.

Simultaneous shear and axial failure, a daunting phenomenon in the context of vertical progressive collapse of R/C frame structures, was briefly examined herein. It seems that a longitudinal reinforcement axial load ratio (axial load over longitudinal reinforcement axial capacity) of 0.65 can be considered an appropriate threshold for its occurrence. Conversely, a ratio equal or higher than 2.00 is associated with such failure. The "grey area" in-between should be further investigated for additional appropriate classification criteria.

Accounting for the effect of different cyclic loading protocols on the post-peak degradation of shear strength is a necessary future step, with a view to properly capturing the effect of cyclic (as opposed to in-cycle) degradation of the shear mechanism. Furthermore, considering a potential non-linear post-peak branch of the shear response curve is deemed a worthwhile effort, which might increase the accuracy in the prediction of this phase of the response. A recommended future endeavour would be to conduct a series of experimental tests with various displacement protocols and put forward a parameter to capture properly the damage caused by continuous displacement reversals, including large displacement reversals as well as low-cycle fatigue.

REFERENCES

[1] H. Sezen, J. P. Moehle, Seismic tests of concrete columns with light transverse reinforcement. *ACI Structural Journal*, **103(6)**, 842–849, 2006.

[2] W. M. Ghannoum, J. P. Moehle, Y. Bozorgnia, Analytical Collapse Study of Lightly Confined Reinforced Concrete Frames Subjected to Northridge Earthquake Ground Motions. *Journal of Earthquake Engineering*, **12(7)**, 1105–1119, 2008.

[3] K. J. Elwood, Modelling failures in existing reinforced concrete columns. *Canadian Journal of Civil Engineering*, **31(5)**, 846–859, 2004.

[4] H. Sezen, Shear deformation model for reinforced concrete columns. *Structural Engineering and Mechanics*, **28(1)**, 39–52, 2008.

[5] M. Baradaran-Shoraka, K. J. Elwood, Mechanical Model for Non Ductile Reinforced Concrete Columns. *Journal of Earthquake Engineering*, **17(7)**, 937–957, 2013.

[6] M. R. Leborgne, W. M. Ghannoum, Calibrated analytical element for lateral-strength degradation of reinforced concrete columns. *Engineering Structures*, **81**, 35–48, 2014.

[7] A. Wibowo, J. L. Wilson, N. T. K. Lam, E. F. Gad, Drift performance of lightly reinforced concrete columns. *Engineering Structures*, **59**, 522–535, 2014.

[8] K. J. Elwood, J. P. Moehle, Axial capacity model for shear-damaged columns. *ACI Structural Journal*, **102(4)**, 578–587, 2005.

[9] J. M. Ricles, Y. S. Yang, M. J. N. Priestley, Modeling nonductile R/C columns for seismic analysis of bridges. *Journal of structural engineering*, **124(4)**, 415–425, 1998.

[10] J. A. Pincheira, F. S. Dotiwala, J. T. D'Souza, Seismic analysis of older reinforced concrete columns. *Earthquake Spectra*, **15(2)**, 245–272, 1999.

[11] P. E. Mergos, A. J. Kappos, A distributed shear and flexural flexibility model with shear–flexure interaction for R/C members subjected to seismic loading. *Earthquake Engineering & Structural Dynamics*, **37(12)**, 1349–1370, 2008.

[12] P. E. Mergos, A. J. Kappos, A gradual spread inelasticity model for R/C beam–columns, accounting for flexure, shear and anchorage slip. *Engineering Structures*, **44**, 94–106, 2012.

[13] P. E. Mergos, A. J. Kappos, Damage Analysis of Reinforced Concrete Structures with Substandard Detailing. *Computational Methods in Earthquake Engineering*, **30**, 149–176, 2013.

[14] P. E. Mergos, Assessment of the Seismic Behaviour of Existing Reinforced Concrete Structures. *PhD Thesis*, Aristotle University of Thessaloniki, Thessaloniki, Greece, 2010. (in Greek)

[15] N. Shirai, B. A. Lejano, H. Adachi, M. Nakanishi, Flexure And Shear Behavior Of High Strength Reinforced Concrete Column Subjected To High And Fluctuating Axial Load. *11th World Conference on Earthquake Engineering*, Acapulco, Mexico, 23-28 June, 1996.

[16] M.R. Leborgne, Modeling the Post Shear Failure Behavior of Reinforced Concrete Columns. *PhD Thesis*, The University of Texas at Austin, Austin, Texas, US, 2012.

[17] K. Henkhaus, S. Pujol, J. Ramirez, Axial Failure of Reinforced Concrete Columns Damaged by Shear Reversals. *Journal of structural engineering*, **139(7)**, 1172–1180, 2013.

[18] K. J. Elwood, J. P. Moehle, Shake table tests and analytical studies on the gravity load collapse of reinforced concrete frames. *PEER Report 2003/01*, University of California, Berkeley, US, November, 2003.

[19] M. Yoshimura, T. Nakamura, Axial collapse of reinforced concrete short columns. *The 4th US-Japan Workshop on Performance-Based Earthquake Engineering Methodology for Reinforced Concrete Building Structures, PEER Report 2002/21*, Toba, Japan, 22–24 October, 187–198, 2002.

[20] A. C. Lynn, J. P. Moehle, S. A. Mahin, W. T. Holmes, Seismic Evaluation of Existing Reinforced Concrete Building Columns. *Earthquake Spectra*, **12(4)**, 715–739, 1996.

[21] H. Ousalem, T. Kabeyasawa, A. Tasai, Evaluation of ultimate deformation capacity at axial load collapse of reinforced concrete columns. *13th World Conference on Earthquake Engineering*, Vancouver, British Columbia, Canada, 2004.

[22] J. Kim, J. Mander, Truss modeling of reinforced concrete shear-flexure behavior. *Technical Report MCEER-99-0005*, Buffalo, New York, US, March 8, 1999.

[23] M. Moharrami, I. Koutromanos, M. Panagiotou, Analysis of shear-dominated RC columns using the nonlinear truss analogy. *Earthquake Engineering & Structural Dynamics*, **44(5)**, 677–694, 2014.

[24] G. A. Chang, Seismic Energy Based Damage Analysis of Bridge Columns. *PhD Thesis*, State University of New York, July, 1993.

[25] H. Ousalem, T. Kabeyasawa, A. Tasai, Effect of hysteretic reversals on lateral and axial capacities of reinforced concrete columns. *5th US-Japan Workshop on Performance-Based Earthquake Engineering Methodology for Reinforced Concrete Building Structures, PEER Report 2003/11*, Hakone, Japan, 10–11 September, 211–221, 2003.

[26] Applied Technology Council, Effects of Strength and Stiffness Degradation on Seismic Response. *FEMA P440A*, Washington, D.C, US, June, 2009.

[27] M. Yoshimura, Formulation of Post-Peak Behavior of old Reinforced Concrete Columns until Collpase. *14th World Conference Earthquake Engineering,* Beijing, China, 2008.

[28] A. B. Matamoros, M. Von Ramin, Estimating the Drift Ratio at Axial Load Failure of Reinforced Concrete Columns on the Basis of a Model to Calculate Shear Strength. *1st NEES/E-Defense Workshop on Collapse Simulation of Reinforced Concrete Building Structures, PEER Report 2005/10,* September, 261–274, 2005.

[29] L. Zhu, K. J. Elwood, T. Haukaas, Classification and seismic safety evaluation of existing reinforced concrete columns. *Journal of structural engineering*, **133(9)**, 1316–1330, 2007.

[30] H. Ousalem, T. Kabeyasawa, A. Tasai, Y. Ohsugi, Experimental study on seismic behavior of reinforced concrete columns under constant and variable axial loadings. *Proceedings of the Japan Concrete Institute,* **24(2)**, 229–234, 2002.

[31] A. B. Matamoros, C. Woods, Drift at Axial Failure of R/C Columns Most Vulnerable to Collapse. *Structures Congress 2010*, Orlando, Florida, US, May 12-15, 2010.